2025 IEEE/SICE International Symposium on System Integration (SII)
January 21-24, 2025, Munich, Germany

Enhancing End-point Accuracy for Path-following Motion of Articulated Redundant Arm

Koki Hasegawa[1], Yuki Shizume[1], Hiroyuki Nabae[1], and Gen Endo[1]

***Abstract*— To enable decommissioning work at the Fukushima Daiichi Nuclear Power Plant, the development of long-reach articulated arms is underway. In decommissioning work, by setting a target path in three-dimensional space and guiding the entire arm along this path, the end effector can reach the target position while minimizing the volume traversed. Therefore, path-following motion is effective for decommissioning work, as it is suitable for passing through narrow spaces and avoiding obstacles. However, conventional methods for calculating target joint angle in path following face the challenge of insufficient end-point accuracy. To improve this accuracy, we propose a target joint angle calculation method that achieves higher accuracy of tip positioning compared to conventional methods. Furthermore, we conducted hardware verifications using the proposed target joint angle calculation method and demonstrated its effectiveness.**

I. INTRODUCTION

The development of long-reach articulated arms for decommissioning work at the Fukushima Daiichi Nuclear Power Plant is progressing [1] [2]. Since the internal space of the nuclear power plant's containment vessel is a high-radiation area, decommissioning work requires operating the arm from outside the containment vessel, where radiation levels are relatively lower, to achieve internal investigation. Therefore, a long and slim articulated arm capable of entering the containment vessel while avoiding obstacles is required, and our research group has developed Mini 3D CT-Arm and Super Dragon [3] [4]. These articulated arms adopt coupled tendon drive proposed by Hirose et al. to support the increasing moment of self-weight associated with the long reach [5].

To investigate the internal conditions of the containment vessel, it is necessary to guide the end effector of the articulated arm to the target position. This requires passing through narrow spaces such as access holes and avoiding obstacles while inserting the arm. Here, as shown in Figure 1, we consider a motion where a moving platform is attached to the base of the articulated arm, and the entire arm follows a target path set in three-dimensional space. By using this path-following motion, the arm can follow the path that the tip has passed through, like a snake, making it suitable for avoiding obstacles and passing through narrow spaces, and thus useful for decommissioning work.

In the path-following motion, it is necessary to calculate the target joint angles of the arm to closely match the target path while advancing. Chirikjian et al. proposed a method to calculate target joint angles for a multi-joint robot composed of serially connected Stewart platforms, where the joints and tip position coincide with the target path by solving inverse kinematics sequentially from the base joint [6]. However, articulated arms such as Mini 3D CT-Arm and Super Dragon are composed of rotational joints, making it impossible to directly apply this method. Yamada et al. proposed a method to set segments corresponding to each joint on the target path and use the deviation angle of each segments as the corresponding target joint angle [7]. However, this method has the issue of insufficient end-point accuracy in articulated arms with fewer joints. In decommissioning work, it is necessary to position the end-point to the target location accurately, so a calculation method with higher accuracy in tip position matching is required.

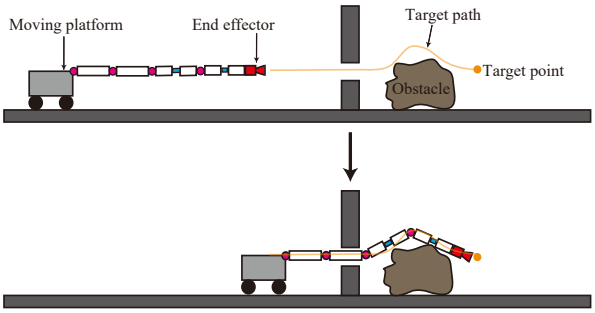

Fig. 1: The path following motion of an articulated arm.

Therefore, the purpose of this paper is to propose a target joint angle calculation method that minimizes the error between the tip position and the target path in the path-following motion of an articulated arm composed of rotational joints. Additionally, we introduce a moving platform to mount the coupled tendon-driven articulated arm Mini 3D CT-Arm, conduct experimental verification of the proposed method, and demonstrate the feasibility of decommissioning work using articulated arms.

II. TARGET JOINT ANGLE CALCULATION METHOD FOR PATH FOLLOWING

In the path-following motion of an articulated arm, it is necessary to control the joint angles to make the arm's pose follow the target path. However, since the articulated arm has a discrete shape, it is impossible to completely match the robot shape to a continuous curved target path. Therefore, it is necessary to calculate target joint angles for the articulated arm that closely match the given target path.

In this chapter, we present previous research on target joint angle calculation methods for path-following motion

[1]All authors are with the Department of Mechanical Engineering, Institute of Science Tokyo, 2-12-1 Ookayama, Meguroku, Tokyo 152-8552, Japan hasegawa.k.ar@m.titech.ac.jp

and their challenges when applied to decommissioning work, and propose a new calculation method that achieves higher accuracy of tip positioning.

Here, it is considered possible to numerically calculate the joint angles such that the tip position and the target path match by solving inverse kinematics using optimization for a general manipulator with redundant degrees of freedom. However, in path-following motion, the most important constraint is that not only the tip but also each joint position must match the target path with good accuracy. Therefore, the authors think that this constraint can be satisfied by sequentially calculating joint angles starting from the root joint to the tip joint.Therefore, we discuss a method for calculating joint angles in accordance with this policy.

In this study, we assume that an end-effector capable of 3-DOF posture control is mounted on the tip of the arm. Therefore, we only consider the accuracy of joint and tip positioning, and do not consider the accuracy of the agreement between the tip orientation. In this paper, we define a joint whose rotation axis is vertical when the arm is extended horizontally as a yaw joint, a joint whose rotation axis is horizontal and perpendicular to the longitudinal direction of the robot as a pitch joint, and rotation around the longitudinal axis of the robot as the roll direction. Also, we refer to the joint positioned at the base side with respect to the advancing direction of the articulated arm as the 1st joint, and sequentially call the joints towards the tip side as the 2nd joint, 3rd joint, and so on.

A. Previous Research

There are mainly two methods proposed for calculating the target joint angles of an articulated robot to follow the target path.

(1) Method to match joint and tip positions to the target path
This method determines the target joint angles so that the positions of each joint and the tip coincide with the target path. Chirikjian et al. calculated the target joint angles as follows to match a manipulator composed of a serial connection of Stewart platforms to a continuous curve [6]. Figure 2 shows this calculation method. In this method, the target positions of each joint are selected on the target path such that the distance between adjacent points is equal to the link length l. The 1st joint is always assumed to be on the target path. For the i-th joint from the 2nd joint onwards, when the target position of the i-th joint is $\boldsymbol{r}_i$, $\boldsymbol{r}_i$ is selected on the target path to satisfy equation (1).

$$\|\boldsymbol{r}_i - \boldsymbol{r}_{i-1}\| = l \tag{1}$$

The target joint angles are calculated by solving inverse kinematics sequentially from the 1st joint to match each joint to the target positions determined by equation (1). This allows the calculation of target joint angles where the positions of each joint and the tip are located on the target path.

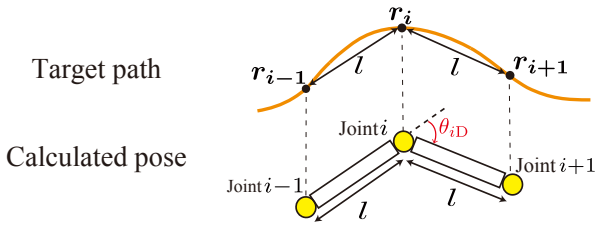

Fig. 2: Chirikjian et al.'s method for calculating the target joint angle of an articulated arm in path following motion.

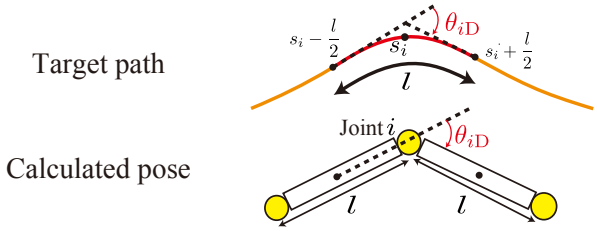

Fig. 3: Yamada et al.'s method for calculating the target joint angle of an articulated arm in path following motion.

(2) Method to use the deviation angle of small sections on the target path as joint angles
This method sets small sections corresponding to each joint on the target path and uses their deviation angles as joint angles. Yamada et al. proposed the following method to accurately match the pose of a snake-like robot to a continuous curve [7]. Figure 3 shows this calculation method. In this method, a coordinate axis s is defined along the target path, and the positive direction of the coordinate axis s is defined as the advancing direction of the robot. Assuming that all joints of the target robot are rotational joints in the same direction and the link length is l, the target angle $\theta_{i\mathrm{D}}$ of the i-th joint is calculated as shown in equation (2).

$$\theta_{i\mathrm{D}} = \int_{s_i - \frac{l}{2}}^{s_i + \frac{l}{2}} \kappa(s) ds \tag{2}$$

Here, the target position s_i of the i-th joint is selected to satisfy $s_i - s_{i-1} = l$. $\kappa(s)$ is the curvature of the target path in the rotation direction of the i-th joint. In this case, $\theta_{i\mathrm{D}}$ is the deflection angle in the rotation direction of the i-th joint over the segments $[s_i - \frac{l}{2}, s_i + \frac{l}{2}]$ on the target path.

We compare these two methods in light of implementation for articulated arms for decommissioning work. In Chirikjian et al.'s previous research, each joint was composed of a Stewart platform, so it was possible to take a pose where all joint and tip positions coincided with the target path. However, articulated arms for decommissioning work such as Mini 3D CT-Arm and Super Dragon are composed of rotational joints, making it impossible to directly apply Chirikjian et al.'s calculation method.

Yamada et al.'s method has the challenge that the tip position is not always on the target path, and in articulated arms with fewer joints, the error between the tip and the target path becomes large. In this research, we aim to guide

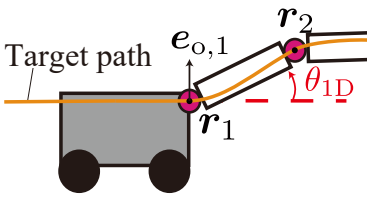

Fig. 4: Proposed method for calculating the target joint angle of an articulated arm in path following motion.

the end effector of the articulated arm to the target position, so it is necessary to accurately match the tip position to the target path.

Thus, previous research on target joint angle calculation methods for path-following motion has challenges when applied to articulated arms for decommissioning work composed of rotational joints.

B. Proposal of a New Target Joint Angle Calculation Method

Based on the previous research mentioned above, we propose a new target joint angle calculation method that minimizes the error between the tip position and the target path to achieve path-following motion for articulated arms composed of rotational joints. First, as shown in Figure 4, the 1st joint is always assumed to be on the target path, and its coordinates in the Cartesian coordinate system are denoted as $\boldsymbol{r_1}$. Next, the target position of the 2nd joint, denoted as $\boldsymbol{r_2}$, is selected on the target path to be located further towards the tip side than $\boldsymbol{r_1}$ and to satisfy $|\boldsymbol{r_2} - \boldsymbol{r_1}| = l$. The target joint angle of the 1st joint can then be calculated using equation (3) to match the 2nd joint to the target path. Here, $\boldsymbol{e}_{o,1}$ is the unit vector perpendicular to both the longitudinal direction as seen from the base and the rotation axis direction of the 1st joint.

$$\theta_{1D} = \sin^{-1}\left(\frac{(\boldsymbol{r_2} - \boldsymbol{r_1}) \cdot \boldsymbol{e}_{o,1}}{\|\boldsymbol{r_2} - \boldsymbol{r_1}\|}\right) \tag{3}$$

For the subsequent joints, the target joint angles are calculated in the same way, sequentially from the base to the top. Specifically, the target angle for the i-th joint is calculated using equation (4). Here, $\boldsymbol{r_i}'$ is the coordinate of the j-th joint, which is the closest joint to the i-th joint on the tip side and rotates in the same direction as the i-th joint. If there is no such joint, the tip coordinate is treated as $\boldsymbol{r_i}'$.

$$\theta_{iD} = \sin^{-1}\left(\frac{(\boldsymbol{r_i}' - \boldsymbol{r}_i) \cdot \boldsymbol{e}_{o,i}}{\|\boldsymbol{r_i}' - \boldsymbol{r}_i\|}\right) \tag{4}$$

In this calculation method, for target paths that curve only in either the pitch or yaw direction, errors will occur for joints in the other direction when calculating the target joint angles. For example, when using this calculation method for a target path that curves only in the pitch direction, all pitch joints and the tip position will be on the target path, but yaw joints will have errors from the target path. Also, in sections of the target path that curve simultaneously in both pitch and yaw directions, errors will occur between the tip position and the target path. Therefore, a target path is designed such that sections with pitch-directional curvature and yaw-directional curvature are divided when considering three-dimensional tip position movements. This design ensures that the tip position achieves a path-following motion with 0 positional error. Although arms with linear motion mechanisms are also useful in decommissioning work [8]. Such arms can also be applied by calculating the target joint angles so that the positions of the rotational joints are aligned on the target path.

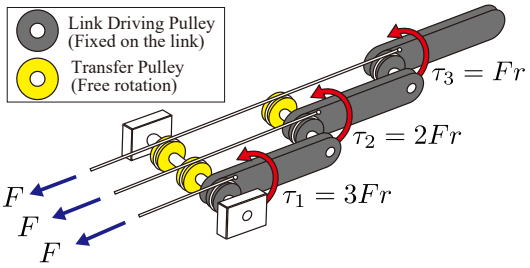

Fig. 5: Coupled tendon-driven articulated arm.

By using this calculation method, it is possible to achieve path-following motion with higher positioning accuracy in tip position, even for articulated arms composed of rotational joints.

III. Mini 3D CT-Arm

This chapter explains the coupled tendon drive, which is the driving method of Mini 3D CT-Arm, and its mechanism.

A. Coupled Tendon Drive

Coupled tendon drive is a driving method for long-reach articulated arms, controlling each joint through actuation by metal wires, ropes, or other tendons [5]. Figure 5 shows an arm composed of three pitch joints driven by coupled tendon drive. Each joint has a drive pulley fixed to the link, and the ends of the tendons are fixed to it. The tendons driving the joints on the tip side are wound around pulleys that can rotate freely on the joints on the base side. Assuming all pulley radii are equal to r and each tendon is pulled with a force F, the torques generated at each joint from the base to the tip are $\tau_1 = 3Fr$, $\tau_2 = 2Fr$, $\tau_3 = Fr$. As shown, the joints closer to the base, which require larger torques to support the self-weight, have more tendons wound around them, enabling the generation of larger torques. Additionally, by mounting the actuators that pull the tendons on the base rather than on the arm, it is possible to reduce the weight of the arm section. In this way, it is possible to support the self-weight of the arm with the tension of multiple tendons, making it suitable as a driving method for long-reach articulated arms.

B. Hardware

Mini 3D CT-Arm is a coupled tendon-driven articulated arm developed by our research group, with an arm length of 2400 mm, and 6 joints (Figure 6). The overall mass is 66.5 kg, the arm mass is 12.1 kg, and the base mass is 54.3 kg. Note that the mass of the base includes the mass of the counterweight that prevents the arm from tipping forward. The arrangement of joints and the length of each link are shown in Figure 7. As shown in Figure 7, the 1st, 2nd, 3rd,

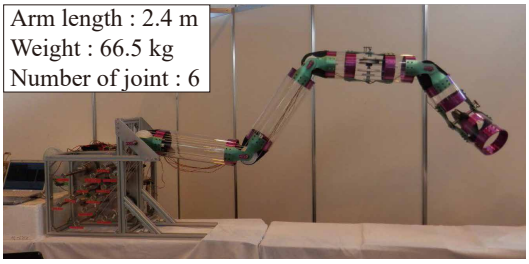

Fig. 6: Coupled tendon-driven articulated arm 'Mini 3D CT-Arm'.

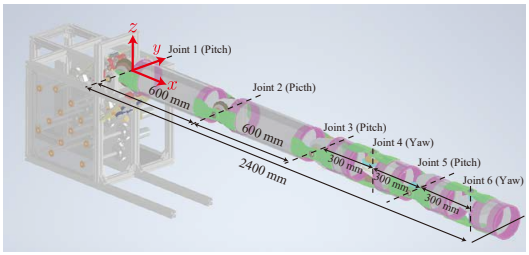

Fig. 7: Direction of rotation and arrangement of the joints of Mini 3D CT-Arm.

and 5th joints rotate in the pitch direction, while the 4th and 6th joints rotate in the yaw direction. This allows the tip of the arm to move in three dimensions. Each joint is driven by heat-set, high-density polyethylene synthetic fiber ropes (NA20020SOC00\001.000, Armare), which are wound and unwound by DC motors mounted on the base. Two ropes are fixed to the drive pulley to pull each joint from both sides, allowing antagonistic actuation of the joints. The joint angle control of the arm is performed by PI control of the winding amount of the drive ropes based on the joint angles measured by potentiometers attached to each joint.

In this paper, we define the x-axis in the longitudinal direction when the arm is extended horizontally, the z-axis in the vertical direction, and the y-axis perpendicular to both the x-axis and z-axis.

IV. Development of the Moving Platform

This section explains the moving platform fabricated to enable movement of Mini 3D CT-Arm. Conventional moving platforms attached to the base of articulated arms include those that push in with linear rails, which have the advantage of excellent base stability because the mechanism is in contact with the ground [9]. In this research, we adopted a method of mounting the base on an omnidirectional moving platform equipped with mecanum wheels. The advantages of adopting an omnidirectional moving platform include excellent stability because the moving platform is in contact with the ground, the ability to fine-adjust the base at the entrance due to omnidirectional movement capability, and the ease of conducting repeated experiments.

Figure 8 shows the fabricated moving platform. Each wheel is driven by a DC motor (148877, Maxon Motor), and the moving platform moves at a constant speed by rotating the DC motors at equal angular velocities. The mass of the moving platform is 11.9 kg, and the maximum

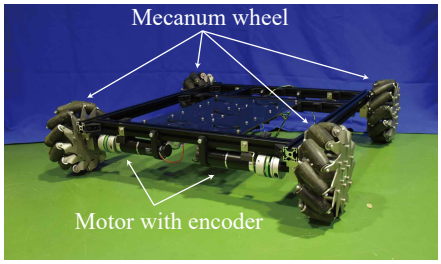

Fig. 8: Omnidirectional moving platform mounted to Mini 3D CT-Arm

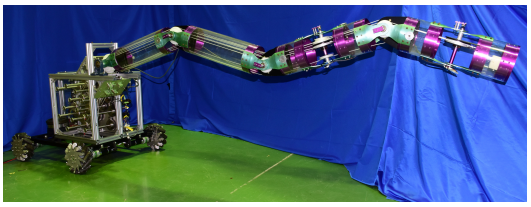

Fig. 9: Mini 3D CT-Arm with the fabricated moving platform attached.

expected movement speed is 100 mm/s. In this study, we conduct path-following motion by driving the moving platform forward along the x-axis. To perform path following, it is necessary for the entire arm to take target joint angles $\boldsymbol{\theta}_{\mathrm{D}}(X_{\mathrm{car}})$ that follow the target path according to the x-coordinate X_{car} of the moving platform. Therefore, rotary encoders were installed on each DC motor of the moving platform. By reading the rotation angle of the wheels with the rotary encoders and multiplying by the radius, it is possible to measure X_{car}. Figure 9 shows Mini 3D CT-Arm with the moving platform attached. This will be used to conduct hardware verification of the target joint angle calculation method for path-following motion.

V. Path Following Experiments

A. Kinematic Simulation

To demonstrate the accuracy of tip positioning using the proposed calculation method, we performed kinematic simulations of path-following motion using MATLAB with the proposed calculation method. We define the target path as a curve in three-dimensional space represented by Equation (5). Here, as mentioned earlier, the coordinate axis along the target path is defined as s, and the target path is described by the curvature in the pitch direction $\kappa_{\mathrm{P}}(s)[\mathrm{rad/mm}]$ and the curvature in the yaw direction $\kappa_{\mathrm{Y}}(s)[\mathrm{rad/mm}]$. Since there are no roll direction joints, the torsion was set to 0.

$$\begin{cases} \kappa_{\mathrm{P}}(s) = -0.002\cos\left(\frac{2\pi}{2400}s\right) \\ \kappa_{\mathrm{Y}}(s) = \begin{cases} 0 & (s < 1500) \\ -\frac{\pi}{1800} & (1500 \leq s) \end{cases} \end{cases} \tag{5}$$

In the simulation, the initial pose of the arm was assumed to be horizontally extended, and we simulated the motion of the tip advancing along the target path from $s = 0$ mm to $s = 2400$ mm. Here, 2400 mm is the arm length of Mini 3D CT-Arm. We also performed a simulation using the joint angle

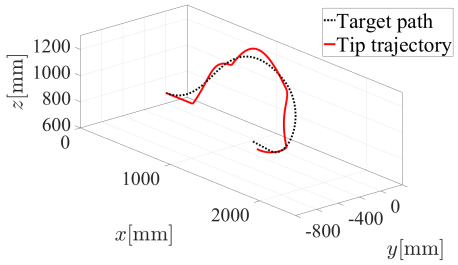

(a) Trajectory when using conventional method [7].

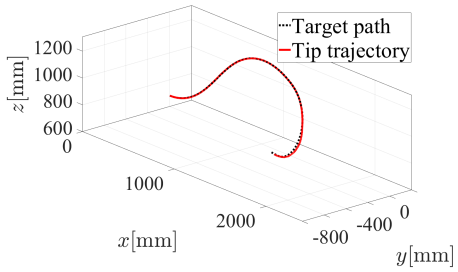

(b) Trajectory when using proposed method.

Fig. 10: Trajectory drawn by tip position in kinematics simulations using MATLAB.

calculation method proposed by Yamada et al., expressed in equation (2), for comparison with the conventional method. In this kinematic simulation, the target path is shown by the black dotted line, and the trajectory drawn by the tip position is shown by the red solid line in Figure 10.

As shown in Figure 10, the proposed calculation method can reduce the error of the tip position compared to the conventional method.

B. Hardware Experiments

We conducted path-following motion experiments using the Mini 3D CT-Arm using the proposed calculation method. We conducted experiments for each of the three paths shown in equations (6) to (8) as target paths. Here, (6) is a path that curves only in the pitch direction, (7) is a path that curves only in the yaw direction, and (8) is a path that curves in the pitch direction for $s < 1500$ and then curves simultaneously in both pitch and yaw directions for $1500 \leq s$.

$$\kappa_{\mathrm{P}}(s) = -0.002 \cos\left(\frac{2\pi}{2400} s\right), \ \kappa_{\mathrm{Y}}(s) = 0 \tag{6}$$

$$\kappa_{\mathrm{P}}(s) = 0, \ \kappa_{\mathrm{Y}}(s) = \begin{cases} 0 & (s < 1500) \\ -\frac{\pi}{2700} & (1500 \leq s) \end{cases} \tag{7}$$

$$\begin{cases} \kappa_{\mathrm{P}}(s) = -0.002 \cos\left(\frac{2\pi}{2400} s\right) \\ \kappa_{\mathrm{Y}}(s) = \begin{cases} 0 & (s < 1500) \\ -\frac{\pi}{1800} & (1500 \leq s) \end{cases} \end{cases} \tag{8}$$

In the initial state, the arm was horizontally extended, and we conducted experiments for each path where the tip position of the arm was advanced from $s = 0$ mm to $s = 2400$ mm at a speed of 20 mm/s, and then retracted from $s = 2400$ mm to $s = 0$ mm at the same speed. Also, the x-coordinate of the 1st joint is defined as the x-coordinate of the moving platform, X_{car}. X_{car} is calculated from the encoder attached to the moving platform's wheel, and the control was performed by determining the target joint angles by substituting X_{car} into the pre-determined target joint angles $\boldsymbol{\theta}_{\mathrm{D}}(X_{\mathrm{car}})$.The results of the experiments for each target path are shown in Figures 11a, 11b, and 11c.

(a) Target path (6)

(b) Target path (7)

(c) Target path (8)

Fig. 11: Hardware experiments of path-following motion.

From the data of each joint angle and moving platform position recorded during the experiment, we calculated the tip position at each time by solving forward kinematics. Figure 12 shows the trajectory drawn by the tip position for each target path. The trajectory drawn by the tip aligns well with the target path, indicating that path following has been achieved. Furthermore, when we calculated the error between the tip position and the target path at each time from this trajectory data, we found that we could achieve a following accuracy within an error range of 120 mm. This maximum error of 120 mm is considered sufficiently small considering that the arm length is 2400 mm.

In this way, we demonstrated the effectiveness of the proposed method in hardware verification when high accuracy of tip positioning is required.

C. Experiment passing through the access hole

To verify the feasibility of decommissioning work using an articulated arm with path-following motion, we conducted the following experiment passing through the access hole. We attempted to guide the tip of Mini 3D CT-Arm to the target position through a through-hole simulating an access hole, using path-following motion. The experimental setup is shown in Figure 13.

The through-hole has a diameter of 300 mm and is installed at a height of 1000 mm from the floor. Since Mini 3D CT-Arm has an arm diameter of 156 mm, the through-hole adequately represents a narrow space. Moreover, the arm height is 681 mm when horizontally extended, so the through-hole is positioned higher than the arm. Therefore,

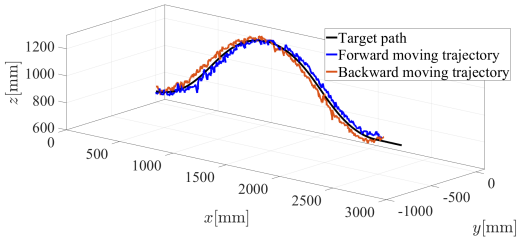

(a) Target path (6)

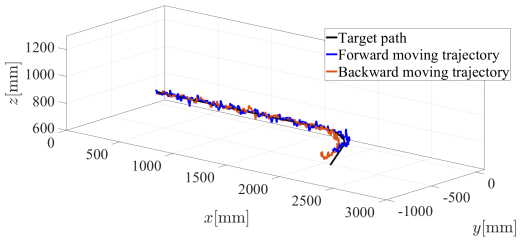

(b) Target path (7)

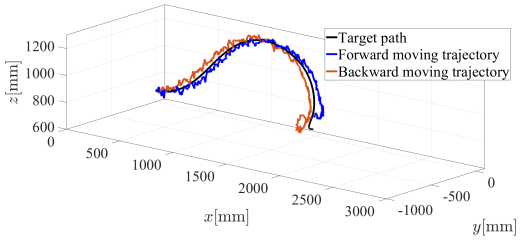

(c) Target path (8)

Fig. 12: Trajectory of the tip with respect to the target path.

this experiment reproduces the motions necessary for decommissioning work, such as passing through narrow spaces and avoiding obstacles.

As a result of the experiment, as shown in Figure 13, we were able to achieve the motion of passing the arm through the access hole and guiding the tip to the target position.

This demonstrates the feasibility of basic motions required for articulated arms in decommissioning work.

VI. Conclusion

In this paper, we proposed a target joint angle calculation method that achieves higher accuracy of tip positioning for path-following motion of articulated arms composed of rotational joints. We also introduced an omnidirectional moving platform to coupled tendon-driven articulated arm Mini 3D CT-Arm and conducted experimental verification of the proposed method, demonstrating that it can follow the target path within an error range of 120mm. Furthermore, we conducted experiment passing through the access hole and demonstrated the feasibility of basic motions necessary for decommissioning work using articulated arms.

In the future, we plan to quantitatively evaluate more accurate path-following accuracy by measuring the tip position using motion capture system.

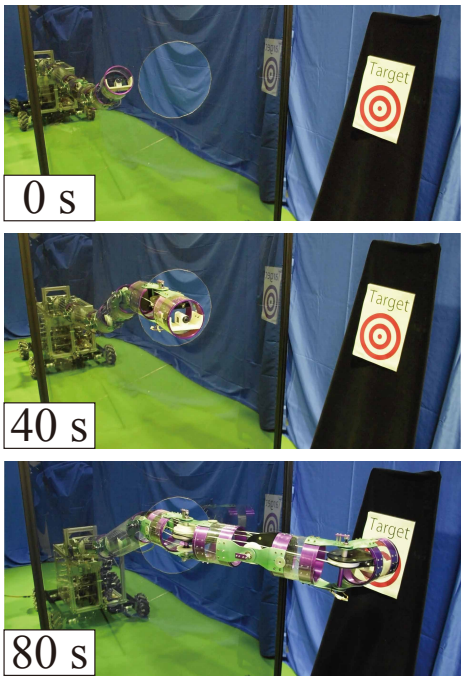

Fig. 13: Result of experiment passing through the access hole. The tip of Mini 3D CT-Arm reached to the target position through a through-hole simulating an access hole.

VII. Acknowledgement

This work was supported by JSPS KAKENHI Grant Number JP22H03668.

References

[1] N. Okuzumi, K. Matsuzaki, and S. Okada, "Development and application of robotics for decommissioning of fukushima daiichi nps by irid," *Journal of Robotics and Mechatronics*, vol. 36, no. 1, pp. 9–20, 2024.

[2] T. Oka, N. Kimura, and S. Hirose, "Truss arm: The world's longest telescopic arm with highest payload and with no deflection for the decommissioning of fukushima daiichi nuclear power plant," in *Advances in Mechanism and Machine Science*, M. Okada, Ed. Cham: Springer Nature Switzerland, 2023, pp. 361–371.

[3] A. Horigome, H. Yamada, G. Endo, S. Sen, S. Hirose, and E. F. Fukushima, "Development of a coupled tendon-driven 3d multi-joint manipulator," in *2014 IEEE International Conference on Robotics and Automation (ICRA)*, 2014, pp. 5915–5920.

[4] G. Endo, A. Horigome, and A. Takata, "Super dragon: A 10-m-long-coupled tendon-driven articulated manipulator," *IEEE Robotics and Automation Letters*, vol. 4, no. 2, pp. 934–941, 2019.

[5] S. Ma, S. Hirose, and H. Yoshinada, "Design and experiments for a coupled tendon-driven manipulator," *IEEE Control Systems Magazine*, vol. 13, no. 1, pp. 30–36, 1993.

[6] G. Chirikjian and J. Burdick, "A modal approach to hyper-redundant manipulator kinematics," *IEEE Transactions on Robotics and Automation*, vol. 10, no. 3, pp. 343–354, 1994.

[7] H. Yamada and S. Hirose, "Study of active cord mechanism (approximations to continuous curves of a multi-joint body)," *J. of the Robotics Society of Japan*, vol. 26, no. 1, pp. 110–120, 2008.

[8] International Research Institute for Nuclear Decommissioning (IRID), "Development of Technology for Investigation inside the Reactor Pressure Vessel (RPV)," [Online]. Available: https://irid.or.jp/wp-content/uploads/2022/08/2021004Fen5final.pdf, Accessed: Jul. 1, 2024.

[9] L. Gargiulo, P. Bayetti, V. Bruno, J.-J. Cordier, J.-P. Friconneau, C. Grisolia, J.-C. Hatchressian, M. Houry, D. Keller, and Y. Perrot, "Development of an iter relevant inspection robot," *Fusion Engineering and Design*, vol. 83, no. 10, pp. 1833–1836, 2008.